Fiber optic Surface Plasmon Resonance sensor based on wavelength modulation for hydrogen sensing

C. Perrotton,[1,*] N. Javahiraly,[1] M. Slaman,[2,3] B. Dam,[4] and P. Meyrueis[5]

[1]*Laboratoire des systemes photoniques, InESS, Universite de Strasbourg, Pole API, Bvd Sebastien Brant, 67400 Illkirch, France*
[2]*Faculty of Sciences, Department of Physics and Astronomy, Condensed Matter Physics, Vrije Universiteit, De Boelelaan 1081, 1081 HV Amsterdam, The Netherlands*
[3]*Delft University of Technology, Department of Chemical Engineering, MECS, Julianalaan 136, 2628 BL Delft, The Netherlands*
[4]*Delft University of Technology, Department of Chemical Engineering, MECS, Julianalaan 136, 2628 BL Delft, The Netherlands*
[5]*Laboratoire des systemes photoniques, Universite de Strasbourg, Pole API, Bvd Sebastien Brant, 67400 Illkirch, France*
**cedric.perrotton@etu.unistra.fr*

Abstract: A new design of a fiber optic Surface Plasmon Resonance (SPR) sensor using Palladium as a sensitive layer for hydrogen detection is presented. In this approach, a transducer layer is deposited on the outside of a multimode fiber, after removing the optical cladding. The transducer layer is a multilayer stack made of a Silver, a Silica and a Palladium layer. The spectral modulation of the light transmitted by the fiber allows to detect the presence of hydrogen in the environment. The sensor is only sensitive to the Transverse Magnetic polarized light and the Traverse Electric polarized light can be used therefore as a reference signal. A more reliable response is expected for the fiber SPR hydrogen sensor based on spectral modulation instead of on intensity modulation. The multilayer thickness defines the sensor performance. The silica thickness tunes the resonant wavelength, whereas the Silver and Palladium thickness determine the sensor sensitivity. In an optimal configuration (NA = 0.22, 100 μm core radius and transducer length = 1 cm), the resonant wavelength is shifted over 17.6 nm at a concentration of 4% Hydrogen in Argon for the case of the 35 nm Silver/ 100 nm Silica/ 3 nm palladium multilayer.

OCIS codes: (130.6010) Sensors; (240.6680) Surface plasmons; (060.2370) Fiber optic sensor.

References and links

1. F. A. Lewis, "Hydrogen in palladium and palladium alloys," Int. J. Hydrogen Energy **21**(6), 461–464 (1996).
2. M. A. Butler, "Optical fiber hydrogen sensor," Appl. Phys. Lett. **45**(10), 1007–1009 (1984).
3. R. R. J. Maier, B. J. S. Jones, J. S. Barton, S. McCulloch, T. Allsop, and J. D. C. Jones, and I. Bennion, "Fibre optics in palladium-based hydrogen sensing," J. Opt. A, Pure Appl. Opt. **9**(6), S45–S59 (2007).
4. M. Tabib-Azar, B. Sutapun, R. Petrick, and A. Kazemi, "Highly sensitive hydrogen sensors using palladium coated fiber optics with exposed cores and evanescent field interactions," Sens. Actuators B **56**(1–2), 158–163 (1999).
5. J. Villatoro, D. Luna-Moreno, and D. Monzon-Hernandez, "Optical fiber hydrogen sensor for concentrations below the lower explosive limit," Sens. Actuators B **110**(1), 23–27 (2005).

#142545 - $15.00 USD Received 11 Feb 2011; revised 24 Mar 2011; accepted 28 Mar 2011; published 16 Sep 2011

6. B. Sutapun, M. Tabib-Azar, and A. Kazemi, "Pd-coated elastooptic fiber optic bragg grating sensors for multiplexed hydrogen sensing," Sens. Actuators B **60**(1), 27–34 (1999).
7. A. Trouillet, E. Marin, and C. Veillas, "Fibre gratings for hydrogen sensing," Meas. Sci. Technol. **17**(5), 1124–1128 (2006).
8. C. L. Tien, H. W. Chen, W. F. Liu, S. S. Jyu, S. W. Lin, and Y. S. Lin, "Hydrogen sensor based on side-polished fiber Bragg gratings coated with thin palladium film," Thin Solid Films **516**(16), 5360–5363 (2008).
9. X. T. Wei, T. Wei, H. Xiao, and Y. S. Lin, "Nano-structured pd-long period fiber gratings integrated optical sensor for hydrogen detection," Sens. Actuators B **134**(2), 687–693 (2008).
10. J. Villatoro and D. Monzon-Hernandez, "Fast detection of hydrogen with nano fiber tapers coated with ultra thin palladium layers," Opt. Express **13**(13), 5087–5092 (2005).
11. X. Bevenot, A. Trouillet, C. Veillas, H. Gagnaire, and M. Clement, "Surface plasmon resonance hydrogen sensor using an optical fibre," Meas. Sci. Technol. **13**(1), 118–124 (2002).
12. C. Perrotton, M. Slaman, N. Javahiraly, H. Schreuders, B. Dam, and Meyrueis, "Wavelength response of a surface plasmon resonance palladium coated optic fiber," Opt. Eng. **50**(1), 014403 (2011).
13. E. Kretschmann, "The determination of the optical constants of metals by excitation of surface plasmons," Z. Phys. **241**, 313–324 (1971).
14. D. Luna-Moreno, D. Monzon-Hernandez, J. Villatoro, and G. Badenes, "Optical fiber hydrogen sensor based on core diameter mismatch and annealed pd-au thin films," Sens. Actuators B **125**(1), 66–71 (2007).
15. M. Slaman, B. Dam, M. Pasturel, D. M. Borsa, H. Schreuders, J. H. Rector, and R. Griessen, "Fiber optic hydrogen detectors containing mg-based metal hydrides," Sens. Actuators B **123**(1), 538–545 (2007).
16. M. Slaman, B. Dam, H. Schreuders, and R. Griessen, "Optimization of mg-based fiber optic hydrogen detectors by alloying the catalyst," Int. J. Hydrogen Energy **33**(3), 1084–1089 (2008).
17. K. Ito and T. Ohgami, "Hydrogen detection based on coloration of anodic tungsten-oxide film," Appl. Phys. Lett. **60**(8), 938–940 (1992).
18. C. Caucheteur, M. Debliquy, D. Lahem, and P. Megret, "Hybrid fiber gratings coated with a catalytic sensitive layer for hydrogen sensing in air," Opt. Express **16**(21), 16854–16859 (2008).
19. M. Mitsushio, K. Miyashita, and M. Higo, "Sensor properties and surface characterization of the metal-deposited spr optical fiber sensors with Au, Ag, Cu, and Al," Sens. Actuators A **125**(2), 296–303 (2006).
20. A. K. Sharma and B. D. Gupta, "Comparison of performance parameters of conventional and nano-plasmonic fiber optic sensors," Plasmonics **2**(2), 51–54 (2007).
21. R. C. Jorgenson and S. S. Yee, "A fiber-optic chemical sensor based on surface plasmon resonance," Sens. Actuators B **12**(3), 213–220 (1993).
22. A. W. Snyder and J. D. Love, *Optical Waveguide Theory* (Springer, 1983).
23. Abeles, "La theorie generale des couches minces," J. Phys. Radium **11**, 307–310 (1950).
24. K. von Rottkay, M. Rubin, and P. A. Duine, "Refractive index changes of Pd-coated magnesium lanthanide switchable mirrors upon hydrogen insertion," J. Appl. Phys. **85**, 408–413 (1999).
25. A. K. Sharma, R. Jha, and B. D. Gupta, "Fiber-optic sensors based on surface plasmon resonance: a comprehensive review," IEEE Sens. J. **7**, 1118–1129 (2007).
26. H. Raether, *Surface Plasmons on Smooth and Rough Surfaces and on Gratings* (Springer-Verlag, 1988).
27. A. Shalabney and I. Abdulhalim, "Electromagnetic fields distribution in multilayer thin film structures and the origin of sensitivity enhancement in surface plasmon resonance sensors," Sens. Actuators A **159**(1), 24–32 (2010).
28. D. Sarid, "Long-range surface-plasma waves on very thin metal-films," Phys. Rev. Lett. **47**(26), 1927–1930 (1981).
29. F. Y. Kou and T. Tamir, "Range extension of surface-plasmons by dielectric layers," Opt. Lett. **12**(5), 367–369 (1987).
30. C. W. Lin, K. P. Chen, C. N. Hsiao, S. Lin, and C. K. Lee, "Design and fabrication of an alternating dielectric multi-layer device for surface plasmon resonance sensor," Sens. Actuators B **113**(1), 169–176 (2006).
31. A. K. Sharma and G. J. Mohr, "Theoretical understanding of an alternating dielectric multilayer-based fiber optic spr sensor and its application to gas sensing," N. J. Phys. **10**, 023039 (2008).
32. V. N. Konopsky and E. V. Alieva, "Long-range plasmons in lossy metal films on photonic crystal surfaces," Opt. Lett. **34**(4), 479–481 (2009).

1. Introduction

Hydrogen detection is an environmental priority for all sustainable energy applications based on hydrogen. Hydrogen is a highly explosive gas in the presence of oxygen. The lower flammability point of hydrogen is 4 % in air and with an upper limit of 74.5%. Being the lightest and the smallest molecule, hydrogen is prone to leak through seals and micro-cracks. This induces security problems to be monitored. In the surrounding of hydrogen based devices, hydrogen

#142545 - $15.00 USD Received 11 Feb 2011; revised 24 Mar 2011; accepted 28 Mar 2011; published 16 Sep 2011

sensors are essential to detect leaks and thus prevent fire and explosion. Optical fibers sensors are very promising devices because of their ability to operate in potentially explosive environments. Most optical hydrogen sensors use a Pd film as a catalyst agent and transducer due to its high catalytic activity and high solubility of hydrogen [1]. Numerous hydrogen fiber sensors (interferometric [2, 3], micro mirror, evanescent sensor [4, 5], Fiber Bragg Grating [6–8] and Long period Grating [9]) have been already proposed. In general, they present a good sensitivity but are limited by (i) their response time and (ii) their cross sensitivity. A nano tapered fiber sensor [10] coated with an ultra thin Pd film was proposed to enhance the response time. In this case, the diffusion of hydrogen is the rate limiting step. However, the fabrication of nano tapered fiber limits the reproducibility and the robustness of such sensors. Surface Plasmon Resonance sensors are an alternative to realize a fast and reproducible hydrogen sensor.

To our knowledge, existing fiber SPR hydrogen sensors are based on intensity modulation. Bevenot et al. [11] presented a Pd- SPR multimode hydrogen fiber sensor. The sensor consists of a Pd layer deposited on a section of the fiber core, after removing the optical cladding. The variation in the palladium complex dielectric permittivity during the hydrogen loading causes a modification of the SPR resulting in a decrease of the loss of the guided light at the Pd reflection interface. They measured the hydrogen concentration by measuring the change in transmitted intensity when the fiber is illuminated by a laser diode with an incidence angle . Nevertheless, the power distribution mode of light in the fiber is very sensitive to mechanical disturbances and fiber impurities. The group mode excited can be disturbed and converted into a other modes. To decrease this effect, we recently presented the response of the Pd-SPR multimode hydrogen sensor [12], where all modes are equally excited in the optical fiber. After a long fiber length (few meters), the power distribution can be considered as uniform. The sensor response showed a change in intensity upon hydrogenation in the wavelength range of 450-900 nm. This change is wavelength dependent, but the sensor does not reveal a spectral resonance. The resonant angle of the SiO_2 /Pd/air observed in the kretschmann configuration [13] is beyond the angle range of the propagating ray. Moreover, we found that the variation in intensity of the Transverse Electric (electric field perpendicular to incidence plane) upon hydrogenation is opposite to that of the Transverse Magnetic (magnetic field perpendicular to incidence plane) polarized light. Although the sensor allows us to measure the hydrogen concentration at several wavelengths, the difference between the TE and TM polarized light in the response decreases the sensitivity of the 'SPR sensor'. It is very challenging to maintain the polarization of the light through the fiber until the transducer region and it demands the use of polarization-controlling elements.

We present, here, the first SPR fiber hydrogen sensor design based on spectral modulation. It replaces the Pd transducer by a multilayer stack made of Ag, SiO_2 and Pd. This structure allow to couple the SP in the NA fiber. Since the SP is only excited for the TM polarization, the structure suppresses the TE influence on the Pd SPR sensor response [12] and takes full advantage of the SP sensitivity. This design can also be applied to other sensitives materials, such as Pd alloys [14] to decrease the cross sensitivity and Mg alloys [15, 16] or tungsten oxide [17, 18] to improve the hydrogen sensitivity (minimum detection pressure, range). We present, here, the principle of the proposed sensor and its optimization.

2. Simulation model

The sensor proposed here consists of a multilayer stack deposited on a section of the fiber core, as drawn in Fig. 1. The multilayer is made of a Ag, a SiO_2 and a Pd layer. Ag is chosen since it is well known as a good candidate for SPR sensors [19]. The Ag layer can be replaced by a Au layer - to avoid the oxidation during the fabrication - or any other metal such as Al or bi-metal [20]. Pd is chosen for its ability to dissociatively split and absorb hydrogen.

In our simulation we consider multimode step index fibers, as in our previous work [12].

#142545 - $15.00 USD Received 11 Feb 2011; revised 24 Mar 2011; accepted 28 Mar 2011; published 16 Sep 2011

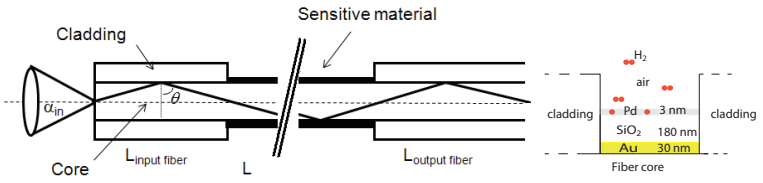

Fig. 1. Schematic representation of the way the sensitive material is deposited on the fiber core, after removing the cladding.

For the fiber Numerical Aperture (NA), the deposit length L and fiber radius r we take 0.22, 1 cm, 100 μm, respectively. We simulate the multimode fiber SPR sensor in a planar approach and consider separately the TE and TM polarizations [21], (-so-called s and p, respectively-). The theory of local plane waves associated to a geometric optics approach is used [22]. The transmitted intensity through the fiber is calculated by summing the power loss/gain at each reflection over the sensitive area. For that, the reflection coefficient is calculated as a function of angle by the transfer matrix method [23]. The total transmitted power I_{out} at a given wavelength λ is defined as:

$$I_{out,\lambda} = 1/2(\int_{\theta_c}^{90} |r_p(\theta)|^{2N} I_{0,\lambda}(\theta_{in}) d\theta + \int_{\theta_c}^{90} |r_s(\theta)|^{2N} I_{0,\lambda}(\theta_{in})) d\theta \quad (1)$$

with:

$$N = L/(D \times tan\theta) \quad (2)$$

where L, D, N are respectively the length of the sensitive area, the fiber diameter and the number of reflections along the sensitive area, while r_s, r_p are the reflection coefficient for polarization TE and TM, respectively. θ defines the angle between the normal of the reflection interface and the direction of the incident light. θ_c is the critical angle. I_0 defines the angular intensity distribution corresponding to the light source used. The distribution is assumed to be uniform simulating a long fiber length. Furthermore the TE and TM polarization are assumed to be equally distributed. Only meridian rays are considered. The model does not take into account scattering from possible roughness of the layer and mode coupling. The normalized intensity is defined as: $I_{out,\lambda} / \int_{\theta_c}^{90} I_0(\theta) d\theta$.

We need the dielectric permitivity of the multilayer system to calculate the reflection coefficient. For this we used the SiO_2 dielectric permittivity given by the Smeiller equation with the Schott industry coefficient as in [12]. For Pd and Pd hydride the experimental dielectric permittivity as obtained by von Rottkay [24] was used. The experimental data of the Pd hydride dielectric permittivity (obtained at 10^5 Pa hydrogen pressure) gives satifiying results compared to the experimental sensor response reported in 4% H_2 in Ar at room condition [12]. The Pd expansion was neglected, which is legitimate for very thin films. In our simulation, we consider the Pd hydride dielectric permittivity corresponding to a concentration of 4% H_2 : the Pd hydride is in the β-phase.

3. Result

3.1. Principle

To demonstrate the principle of the sensor, we simulate the 35 nm Ag / 180 nm SiO_2 / 3 nm Pd multilayer stack. Figure 2 reveals the transmitted intensity of the optical fiber. The sensor response shows a spectral resonance peak in contrast to the Pd SPR fiber sensor in which the Pd layer is deposited on the fiber core as shown in Fig. 2(b). Upon hydrogenation, the resonant

#142545 - $15.00 USD Received 11 Feb 2011; revised 24 Mar 2011; accepted 28 Mar 2011; published 16 Sep 2011

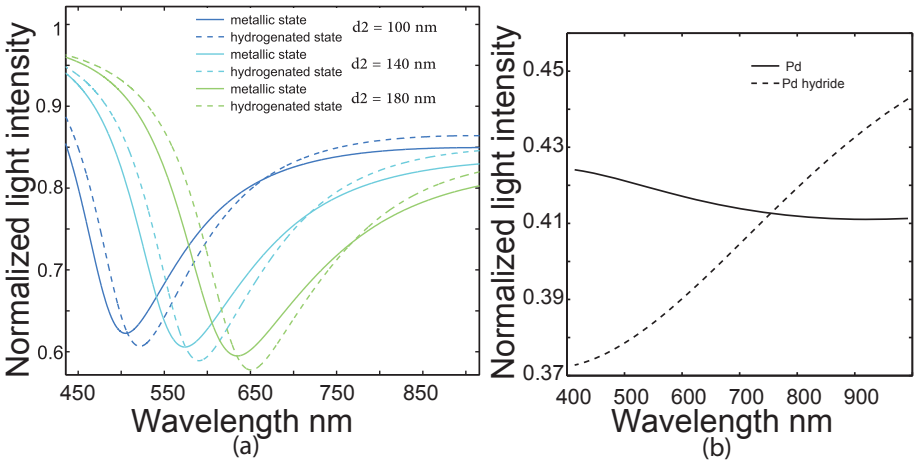

Fig. 2. (a) The transmitted light intensity as a function of the wavelength for different thickness of SiO_2. The transducer is a multilayer composed of 35 nm Ag / d2 nm SiO_2/ 3 nm Pd. (NA = 0.22, core radius = 100 μm, L = 1 cm). (b) The transmitted light intensity as a function of the wavelength, where the transducer is a 10 nm Pd layer (NA = 0.22, core radius = 100 μm, L = 2 cm)

wavelength shifts to higher wavelengths. The observed peak corresponds to the excitation of the SP. The first metal layer made the sensor insensitive to the TE polarization since the SP is only coupled by TM polarized light. The TE polarized light is reflected without being affected by the change in the surrounding index as shown in Fig. 3(a). Roughly speaking, the Au layer prevents the TE- polarized wave from reaching the sensing medium (here the Pd layer) due to the ohmic loss in the metal layer as it is commonly observed in the Au SPR fiber index refractive sensor [25]. The transmitted intensity through the fiber is therefore only determined by the reflection coefficient of the TM polarized light for the propagating rays. When the resonance condition of the SP is fulfilled, a sharp dip in transmitted intensity is observed. In our multilayer structure, the resonance condition occurs when the evanescent wave (*kev*) (generated from the incident light) matches with the propagation constant β of the SPW. β is determined from the dispersion relation of the corresponding multilayer waveguide. Upon hydrogenation, the propagation constant β is altered due to the decrease in the both parts of the Pd complex dielectric permittivity. The position (related to real component of β) and the shape of the SPR (related to imaginary component of β) is therefore changed. Furthermore, the variation of the partially reflected field at the SiO_2/Pd and Pd/air interface upon hydrogenation affects the interference between the incoming and the reflective wave. The hydrogenation of Pd changes the electromagnetic field distribution inside the multilayer. As emphasized by Pockrand and Raether [26], the depth of the SPR minimum is related to the field distribution and determined by the ratio of the intrinsic and radiation damping. Therefore, the minimum of the SPR peak changes, here, upon hydrogenation. Figure 3(a) shows the electric field distribution inside the multilayer for wavelengths of 670 nm and 855 nm. The electric fields are plotted at the resonant angle of $\theta_{SPR,Pd}$ for the both metallic and hydrogenated states, respectively. Figure 3(b) shows the SPR reflectance curves. At resonance, the electric field intensity is maximum at the SiO_2/Pd interface for the short wavelengths. This wavelength distribution is opposite to the penetration depth distribution. This is explained by the optical metal properties: the metal is more transparent and less absorbing for the blue than the red wavelength, as emphasized by Shalabney et

#142545 - $15.00 USD Received 11 Feb 2011; revised 24 Mar 2011; accepted 28 Mar 2011; published 16 Sep 2011

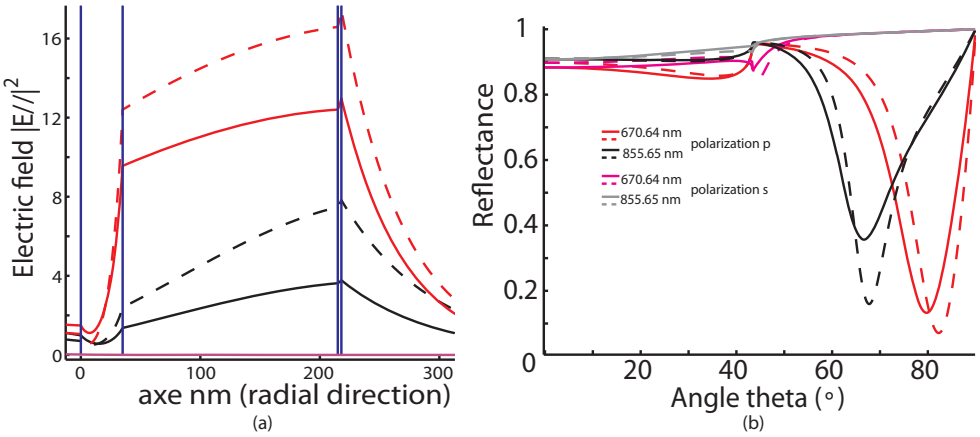

Fig. 3. (a) The electric field ($E_{//}$) distribution into a multilayer made of 35 nm Ag / 180 nm SiO_2 / 3 nm Pd for the metallic (line) and hydrogenated state (dash line) at the resonance ($\theta_{SPR,Pd} = 79.73°$ and 66.68° for λ =670.64 nm (red and pink for polarization p and s, respectively) and 855.65 nm (black), respectively). (b) Reflectance as a function of the angle theta (0° corresponds to the normal incidence) for p and s-polarization at different wavelengths.

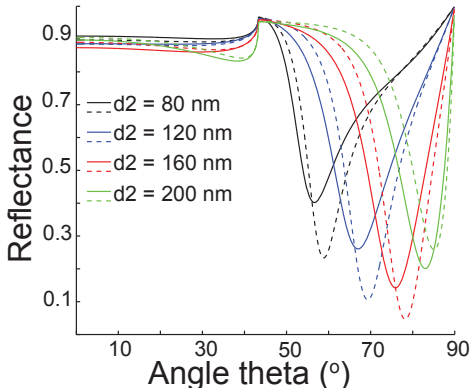

Fig. 4. Reflectance of a multilayer made of 35 nm Ag / d2 nm SiO_2 / 3 nm Pd for a wavelength of 670 nm. The lines and dash lines represent the metallic and hydrogenated state, respectively.

al. [27]. Figure 3(a) shows that the electric field increases upon hydrogenation at the SiO_2/Pd interface. The hydrogenation of the Pd layer indeed makes the metal more transparent and less absorbing.The electric field is then redistributed into the multilayer and consequently, the SPR curve is altered.

3.2. Choice of the layer thicknesses

The thicknesses of the silver (d1), silica (d2) and Pd (d3) layers as well as the ratios of the thickness define the resonance conditions and the performances of the SPR sensor. The performance of a SPR fiber sensor based on spectral modulation is described in terms of the sensitivity S and the signal-to-noise ratio (SNR). The first defines, here, the shift of the resonant wavelength $\delta\lambda_{res}$ due to a concentration of 4 % hydrogen. The second is inversely proportional to the full

#142545 - $15.00 USD Received 11 Feb 2011; revised 24 Mar 2011; accepted 28 Mar 2011; published 16 Sep 2011

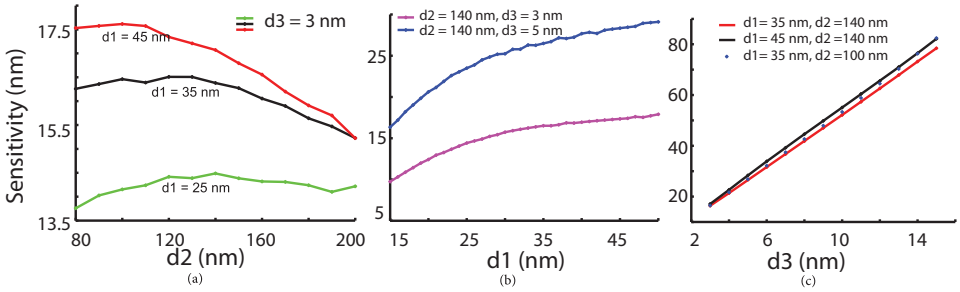

Fig. 5. Sensitivity as function of (a) the SiO_2 thickness for different Ag thicknesses, (b) of the Ag thickness for different Pd thicknesses and (c) of the Pd thickness for different Ag and SiO_2 thicknesses.

width at half-maximum (FWHM) corresponding to the SPR ($SNR = \delta\lambda_{res}/\delta\lambda_{FWHM}$). FWHM should be as small as possible to get the best resolution.

For the intermediate SiO_2 layer, we require that it is thin enough to avoid multi modes in the Metal Insulator Metal waveguide (MIM) and thick enough to decouple the SP (supporting by Ag and Pd). It is used to position the resonance into the angular range of the fiber. By increasing the thickness of the SiO_2 layer, the effective index ($n = \beta/k_0$) of the SP increases, i.e the resonance position is shifted to greater angles at a given wavelength, as depicted in Fig. 4. The choice of the SiO_2 thickness allow us to define the resonant wavelength in the sensor response, as shown in Fig. 2(a). It shifts toward the long wavelengths with increasing the SiO_2 thickness. The minimum of the peak changes as the radiation damping is affected. The peak widens at longer wavelength due to the increase of the metal absorption. Nevertheless, the sensitivity, as depicted in Fig. 5, and the SNR are weakly altered by the silica thickness compared to the silver and Pd thicknesses. (The irregularity on the sensitivity curves is due to the wavelength discretization pitch in the simulation).

Increasing the Pd thickness widens the resonance peak and increases the peak minimum value, as shown in Fig. 6(a). The absorption of Pd causes the broadening of the resonance. The change of the resonance depth is related by the change in the ratio of the two damping processes. It is worth noting that an increasing Pd thickness shifts the SPR peak toward shorter wavelengths due to the decrease of the effective index of the SP. Figure 5(c) shows the sensitivity increases with increasing the Pd thickness. A trade off has to be found between the sensitivty and the SNR. A 3nm Pd thickness appears appealing to conceive a fast and reproducible hydrogen sensor.

Figure 5(b) shows that the sensitivity increases with the Ag thickness. However, the peak minimum is negatively affected due the radiation damping, and the SNR decreases with increasing the Ag thickness, as depicted in Fig. 6(b). The resonant wavelength is also shifted to the longer wavelengths.

4. Discussion

In our design, the NA, the core diameter and the deposit length play a crucial role in the performance of the sensor. As previously reported for the SPR fiber sensor: an increase of the number of reflections decreases the value of the minimum peak, but trends to widen the peak; a decrease of the NA gives a narrower SPR peak, as depicted in Fig. 7. Therefore, we choose a value of 0.22 for the NA and 1 cm for L, with a core radius of 100 μm. According to our simulation, for a multimode step index, we find that the 35 nm Ag/ 100 nm SiO_2/ 3 nm Pd multilayer is the optimal design to obtain the best trade-off between the sensitivity and the SNR.

#142545 - $15.00 USD Received 11 Feb 2011; revised 24 Mar 2011; accepted 28 Mar 2011; published 16 Sep 2011

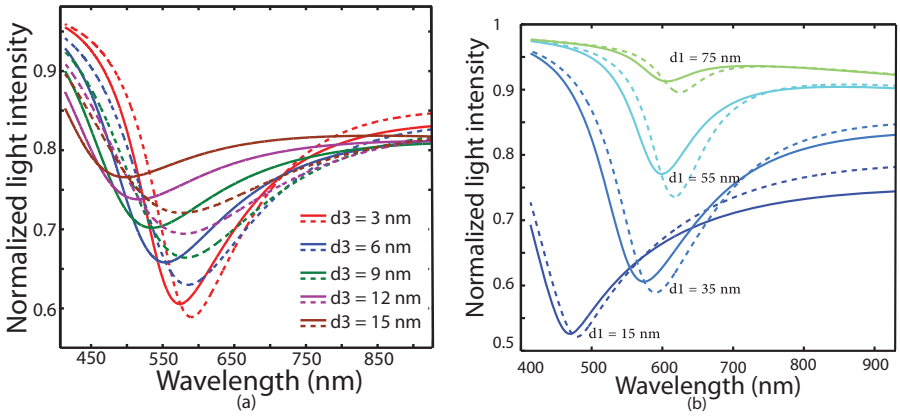

Fig. 6. Normalized light intensity as a function of the wavelength for (a) different thickness (d3) of Pd and (b) different thickness (d1) of Ag. The transducer is a multilayer made of d1 nm Ag / d2 nm SiO_2 / d3 nm Pd. (NA = 0.22, core radius = 100 μm, L = 1 cm). The lines and dash lines represent the metallic and hydrogenated state, respectively.

Regarding the sensitivity, the resonant wavelength shows a shift of 17.6 nm at a concentration of 4% H_2 in Ar (NA =0.22, L=1cm, core radius=100 μm, 35 nm Ag/ 100 nm SiO_2/ 3 nm Pd). Although further investigations have to be done in order to estimate the wavelength shift as a function of the hydrogen concentration, the large sensor response makes us confident that a reliable hydrogen response will also be obtained at lower hydrogen concentrations. We expect that the sensitivity (i.e the shift of the resonant wavelength) will not be significantly altered by the intensity fluctuation/modal distribution of the light, contrary to the fiber SPR hydrogen sensor based on the intensitity modulation. In order to improve the sensitivity or the minimum level of detection, the Pd layer can be replaced by any sensitive material to hydrogen presenting a optical change. The proposed design does not explicitly use the SPR of the Pd, but its ability to change the surrounding index medium. Sensitive material such as Pd alloys, Pd nanoparticles inserted in a substrate matrix, oxide materials (WO_3, Pd_2VO_5) or Mg alloys with a cap layer of Pd could be envisaged.

Regarding the SNR of the sensor, we could envisage to deposit a Pd fim of a thickness below 3 nm to decrease the broad SPR peak. Further investigations have to be done to claim this point since below 3 nm Pd does not form a closed film and the dielectric permittivity used in our simulation is not validated for a Pd island film. Adding an intermediate dielectric layer before the silver layer (Long range SP [28, 29]) or a Bragg multilayer system [30–32] made of TiO_2/SiO_2 could be another possible way to enhance the sensor SNR.

5. Conclusion

We have proposed a SPR fiber hydrogen sensor based on wavelength modulation. The sensor is only sensitive to TM polarized light. TE polarized light is now used as a signal reference. A more reliable response is expected for such a multimode fiber SPR hydrogen sensor based on spectral modulation as compared to the ones based on intensity modulation. The operating wavelength is tuned by adjusting the intermediate layer thickness. A multi-point sensor could be realized by adding Fiber Bragg grating after each sensing region.

#142545 - $15.00 USD Received 11 Feb 2011; revised 24 Mar 2011; accepted 28 Mar 2011; published 16 Sep 2011

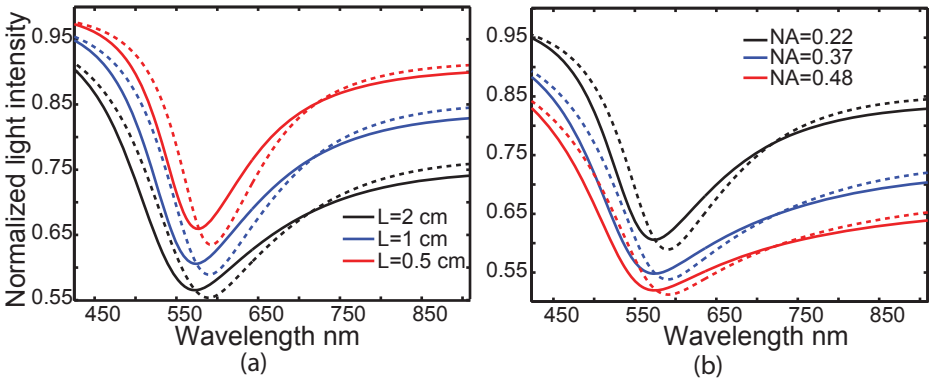

Fig. 7. Normalized light intensity as a function of the wavelength for (a) different lengths (the core radius, and the NA is 100 μm and 0.22, respectively) for (b) different fiber NA (the core radius, and the deposit length is 100 μm and 1 cm, respectively). The transducer layer is made of 35 nm Ag / 140 nm SiO_2 / 3 nm Pd. The lines and dash lines represent the metallic and hydrogenated state, respectively.

Acknowledgments

The authors would like to thank P. Pfeiffer for useful discussion. We acknowledge financial support from the Nederlandse Organisatie voor Wetenschappelijk Onderzoek NWO through the Sustainable Hydrogen Programme of Advanced Chemical Technologies for Sustainability program. The funding from the Region Alsace in France is gratefully acknowledged.

#142545 - $15.00 USD Received 11 Feb 2011; revised 24 Mar 2011; accepted 28 Mar 2011; published 16 Sep 2011